Journal of Microscopy, Vol. 226, Pt 1 April 2007, pp. 1–5
Received 15 September 2006; accepted 3 January 2007

LED illumination for video-enhanced DIC imaging of single microtubules

VOLKER BORMUTH*, JONATHON HOWARD*
& ERIK SCHÄFFER*†
* *Max Planck Institute of Molecular Cell Biology and Genetics, Pfotenhauerstraße 108, 01307 Dresden, Germany*

Key words. DIC, differential interference contrast, LED, light emitting diode, microtubules, optical tweezers, video-enhanced.

Summary

In many applications high-resolution video-enhanced differential interference contrast microscopy is used to visualize and track the ends of single microtubules. We show that single ultrabright light emitting diodes from Luxeon can be used to replace conventional light sources for these kinds of applications without loss of function. We measured the signal-to-noise ratio of microtubules imaged with three different light emitting diode colours (blue, red, green). The blue light emitting diode performed best, and the signal-to-noise ratios were high enough to automatically track the ends of dynamic microtubules. Light emitting diodes as light sources for video-enhanced differential interference contrast microscopy are high performing, low-cost and easy to align alternatives to existing illumination solutions.

Introduction

Video-enhanced differential interference contrast was first introduced by Allen *et al*. (1981). The technique benefits from its ability to visualize sub-resolution phase objects, such as single 25-nm-diameter microtubules, and its sharp sectioning capability in comparison to phase contrast or dark field microscopy (Allen *et al.*, 1981; Inoue, 1981, 1989; Salmon & Tran, 1998). The major problem for the optimization of video-enhanced differential interference contrast microscopy (VE-DIC) was to find a stable, intense, incoherent and uniform light source with a narrow bandwidth. Ellis solved this problem in 1985 by introducing a fibre optic light scrambler that transforms the non-uniform light emission from an arc lamp into a uniform light disk that homogeneously fills the condenser back aperture (Inoue & Spring, 1997). VE-DIC was used, for example, to study microtubule mechanics, protein regulation of microtubule dynamics and microtubule based-motor proteins (Allen *et al*., 1985; Salmon, 1995; Dogterom & Yurke, 1997; Kinoshita *et al*., 2001). In these studies, VE-DIC was preferred over fluorescent microscopy because it does not suffer from bleaching or out-of-focus fluorescence.

Parallel to the developments of VE-DIC, light emitting diodes (LEDs) have evolved from dim indicator lamps to bright and stable light sources with the possibility of fast, microsecond switching. Generally, blue LEDs are brightest and green LEDs are dimmest (Goetz, 2003; Gross, 2005). In microscopy, more and more studies show that LEDs can replace conventional lamps for fluorescence applications (Herman *et al*., 2001; Silk, 2002; Haseloff, 2003; Labvision, 2005; Moser *et al*., 2006). Commercial producers are beginning to offer LED illumination for bright field microscopy (Zeiss, 2005; Boreal.com, 2006); however, these implementations have not been demonstrated to be capable of resolving sub-resolution phase objects.

For this study, we developed a simple and compact LED condenser. The setup is suitable for visualizing single microtubules and their dynamics. The low heat emission of the LEDs also reduces thermal drift and therefore makes our condenser ideal in combination with other single molecule techniques such as optical tweezers.

Methods

The LED-VE-DIC is implemented on an inverted Zeiss Axiovert 135 TV microscope (Zeiss, Germany). The microscope arm that normally holds the bright field light source was removed and the original condenser replaced by our stand-alone condenser (Fig. 1). The condenser sits on the static part of the microscope stage on three fine-adjustment screws that allow for height adjustment. The LED is mounted on a heat sink with a

†Current address: Center of Biotechnology, Technical University Dresden, Tatzberg 47-51, 01307 Dresden, Germany

Correspondence (including request for programs) to: Volker Bormuth. Tel.:; fax:; e-mail: bormuth@mpi-cbg.de

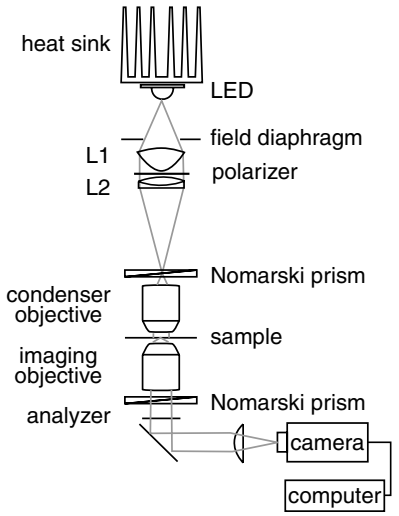

Fig. 1. Schematic illustration of the LED based video-enhanced DIC setup.

thermal resistance of 1.75 K/W that is thermally insulated from the rest of the condenser. Next on the optical path is a field-iris, a collimating lens L1 [anti-reflection (AR) coated, aspheric condenser lens, diameter $d = 31.5$ mm, focal length $f = 27$ mm], a dichroic sheet polarizer, an imaging lens L2 (AR-coated achromat, $d = 25.4$ mm, $f = 80$ mm), a Nomarski prism, and a strain-free condenser objective suitable for DIC (Zeiss Plan-Neofluar 40×, 1.3 NA, oil immersion). All parts but the condenser objective are mounted on four rods (Microbench system, LINOS Photonics, Germany) that are fixed on a thick aluminium base plate. This allows for free vertical positioning of all components. In addition, the LED, the iris and the complete condenser are laterally adjustable. In total, the degrees of freedom are sufficient to achieve Köhler illumination. The custom-built condenser has a height of 23 cm. On the imaging side, a Zeiss Plan-Neofluar 100×, 1.3 NA, oil-immersion objective is used. VE-DIC is realized with a standard video camera (LCL-902HS Watec, Japan, pixel size 8.6 μm × 8.3 μm, 735 × 572 pixel^2, frame rate $f_{\text{video}} = 25$ Hz). An adjustable zoom before the camera was used for all acquired images to double the magnification. The frames are acquired with a video card with adaptable gain and offset of the A/D preamplifier (NI-PCI-1407, 8-bit, National Instruments, Austin, TX USA). A previously stored background image is subtracted and an average over a user-defined number N of adjacent images is calculated. The overall intensity variation of the background image was typically on the same order of magnitude as the signal of the microtubules. The processed images are displayed and stored at a rate of f_{video}/N. Image processing is performed with custom written software (Labview7.1, National Instruments).

We tested a blue, a green, and a red Luxeon star LED (Lumileds Lighting, San Jose, CA, USA; Table 1). We found that the LED's could be stably operated up to a current of $I \lesssim 2$ A. Up to this current, the LED intensity steadily increased. Before implementing LEDs in a setup, several LEDs of the same colour should be compared to choose the brightest one, since LEDs from the same batch can vary by up to a factor of 3 in intensity (Benavides & Webb, 2005).

All samples were prepared in a flow cell constructed of two No. 1.5 cover glasses (Corning) separated by two Parafilm strips placed next to each other. The 3-mm spacing between the strips forms a channel. The Parafilm is shortly melted on a hot stage to seal the channel walls. This results in a channel height of 100 μm and a total thickness of the flow cell of 440 μm.

For the experiments with dynamic microtubules, rhodamine-labelled microtubule seeds were grown for 30 min at 37°C (6 μM rhodamine-labelled tubulin, 1 mM GMP-CPP, 1 mM $MgCl^2$, BRB80 [80 mM PIPES/KOH pH 6.9, 1 mM $MgCl^2$, 1 mM EGTA]). They were immobilized with rhodamine antibodies on the surface of a flow cell. Microtubule assembly was initiated by perfusion of 20 μL reaction mix into the flow cell (1 mM GTP, 0.1 mg/mL BSA, 1 mM MgCl2, 75 mM KCl, 12.5 μM non-labelled tubulin, BRB80). All experiments were performed at 25°C.

Tracking, image processing, and analysis were performed off-line. For automatic tracking we used custom written Labview7.1 code. A small region of interest was selected around the microtubule end and automatically tracked by pattern recognition in consecutive images. The manual tracking was performed by mouse clicking on the microtubule end in each image with software written by N. Carter (retrac.exe, http://mc11.mcri.ac.uk/Retrac/index.html). Some images were processed with a Fourier band-pass filter for structures <2 pixels and >50 pixels (ImageJ, http://rsb.info.

Table 1. Luxeon LED specifications

Colour	Electrical power (W)[a]	$\Delta\lambda$ (nm)	$\Delta\lambda$ (nm)	Light power (W)[a]	Current I (A)[b]	Emitter area (mm^2)[c]	Model
Blue	4.8	450	20	0.70	0.7	4	LXHL-LR5C
Green	4.8	535	35	0.26	0.7	4	LXHL-LM5C
Red	4.1	630	20	0.77	1.4	1	LXHL-LD3C

[a]Power at recommended maximum operating current.
[b]Recommended maximum operating current.
[c]Benavides & Webb, 2005.

nih.gov/ij/). The signal-to-noise ratio (SNR) in the images was obtained from rectangular regions of $n \times m$ pixel^2. We averaged the signal over $m = 10$ lines and calculated the SNR as the ratio of the peak-to-peak difference of the averaged signal divided by the standard deviation of the background noise from the rectangular region. Note that the line averaging only reduces the error on the mean signal. The noise value is *not* based on line-averaged values. The error on the SNR was calculated from the relative standard deviation of the noise and the standard error of the mean of the signal. SNRs were all measured with microtubules oriented perpendicular to the DIC shear axis. In shot-noise limited images, the SNR scales with the square root of the light intensity – thus, approximately with the square root of the LED operating current ($\sqrt{\mathrm{I}}$) – and with the square root of the number of averaged images ($\sqrt{\mathrm{N}}$).

Results

With all three LEDs (blue, green and red, see Table 1), we visualized single microtubules. Qualitatively, by inspection with the eye, the use of the blue LED produced the best images. An advantage of the blue LED was that the microtubules appeared narrower due to the smaller point spread function at shorter wavelengths. To quantify the image quality, we measured the signal-to-noise ratio (see Methods), defined as the peak-to-peak signal from the microtubule divided by the root-mean-square noise. With the blue LED we achieved the highest SNR, which allowed us to visualize single microtubules with video-rate (25 Hz) and a SNR of 3.4 ± 0.2 (LED current $I_{\max} = 2$ A, Fig. 2a). The SNR could be further improved by image processing. Applying a Fourier filter to the image in Fig. 2a increased the SNR by a factor of 2.9 (data not shown). Averaging over $N = 25$ consecutive images resulted in a SNR $= 9.5 \pm 0.4$ of the averaged image (Fig. 2b). By applying the Fourier filter to the averaged images, the SNR increased further to SNR $= 14.8 \pm 0.1$ (Fig. 2c). Microtubules were also clearly visible (data not shown) with a green (SNR $= 3.1 \pm 0.3$, $I = 0.75$ A) and a red LED (SNR $= 4.1 \pm 0.6$, $I = 0.6$ A) when 25 frames were averaged. Given the fact that the red LED has a smaller emitter area (Table 1), therefore a higher luminous density, and consequently a higher irradiance in the field of view (conserving étendue), we expected a higher SNR for the red LED compared to the blue one, after taking the different operating currents into account. The lower SNR could be due to the large variability in light output of LEDs (see Methods and Benavides & Webb, 2005). Furthermore, the width of the point spread function and Rayleigh scattering favour blue LEDs.

An arc lamp adjusted in critical illumination for VE-DIC produced comparable SNRs (Kinoshita *et al.*, 2001). We analyzed data from Kinoshita *et al.* and found that the SNR $= 4.8 \pm 0.3$ for a single frame (corrected for the different magnification used). This is only slightly larger than our value of 3.4 obtained with the blue LED.

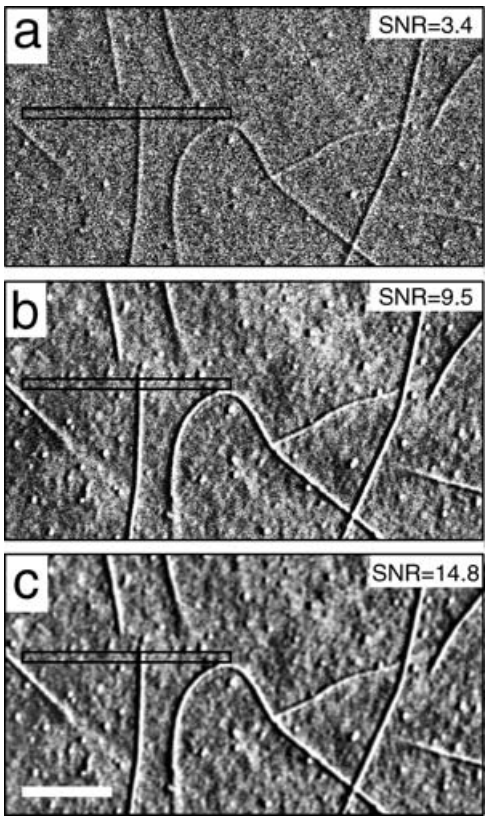

Fig. 2. Background-subtracted video-images show microtubules that are immobilized on a hydrophobic silanized glass surface (a–c). Image (a) is a single frame acquired at video-rate, image (b) is the average over 25 consecutive frames of the same region and image (c) shows image (b) after application of the Fourier band-pass filter. All images were acquired with the blue LED and a 200× magnification (100× objective plus 2-fold zoom). The scale bar corresponds to 5 μm (a–c). The region indicated by a black box was used to calculate the signal-to-noise ratio (SNR) indicated in each image.

The SNRs from our LED setup were sufficient to image growing and shrinking microtubules, and to quantify their end dynamics with an automatic tracking routine based on pattern recognition. A tracking result is shown in Fig. 3. The automatic tracking routine returned the end position with a standard deviation of 59 nm (black line, Fig. 3). For comparison, we analyzed the image sequence manually by mouse clicking (gray line, Fig. 3). The automatic and manual tracking results are consistent with each other and the microtubule poly and depolymerization velocities agree well with previously published measurements (Fygenson *et al.*, 1994; Mitchison, 1994).

Discussion and conclusion

In general, LEDs are not yet as bright as arc lamps. Nevertheless, they show comparable, surprisingly high performance in our VE-DIC setup. This is mainly due to the

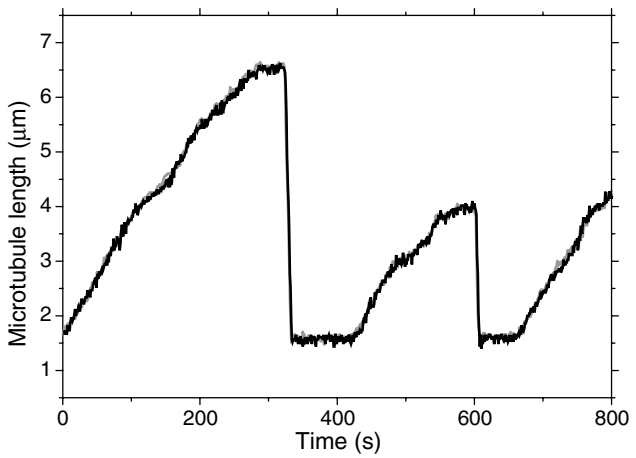

Fig. 3. End tracking of a single dynamic microtubule. The black line shows the result from the automatic tracking based on a pattern recognition algorithm. The grey curve corresponds to the average over two data sets obtained by manual end tracking of the microtubule. The images used in the analyses were obtained with a green LED (SNR $= 9.4 \pm 0.3$, $N = 25$, Fourier filter, $I = 0.75$ A).

fact that, with LEDs, high quality Köhler illumination with narrow bandwidth can be established with minimal light loss along the illumination path. Light loss is minimized since optical elements, such as fibre optics, holographic diffusers, band-pass, or heat filters, are not necessary in the condenser setup. The presented LED-VE-DIC is a high-performing, low-cost VE-DIC solution that is furthermore simpler to align due to the small number of optical elements used compared to other illumination solutions. In addition, the LED light intensity is very stable which facilitates background subtraction and data analysis. The coefficient of variation of the LED intensity measured with a photodiode over a period of 1 min with 25 Hz was 0.02%. The LEDs did not show any spikes in the intensity traces that are sometimes observed in traces from arc lamps. Therefore, intensity fluctuations did not affect our measurements.

For our applications, the LED-VE-DIC turned out to have further advantages due to its low heat emission. This allowed us to use it in combination with optical tweezers (Schäffer *et al.*, 2007) to reduce thermal drift, which is detrimental during single molecule experiments with nanometre precision (Neuman & Block, 2004). With 5 W of electrical power used by the LED illumination, we reduced temperature gradients in the room significantly compared to illumination solutions with 100 W arc or halogen lamps (Carter & Cross, 2001). Furthermore, the long lifetime of the LED allows long-term temperature equilibration. In the equilibrated setup, the temperature of the sample and the objectives varied by less than 0.1 K per h (Schäffer *et al.*, 2007).

For the high light intensity of the blue LED, images were not shot-noise-limited anymore for a bandwidth of $\lesssim 1$ Hz. The improvement in the SNR of Fig. 2b compared to Fig. 2a by a factor of 2.8 due to the averaging was smaller than the expected factor of 5 ($=\sqrt{25}$). The reason for this is that surface structures and impurities, with a signal larger than the background noise were resolved in Fig. 2b next to the microtubules. Based on the signal of these structures relative to the microtubule, the surface features must be on the order of $\lesssim 1$nm thick.

In summary, we have shown that LEDs provide adequate illumination for video-enhanced DIC.

Acknowledgments

We thank A. A. Hyman for helpful discussions, Kazuhisa Kinoshita and Isabelle Arnal for providing arc lamp data, Michel Volkmer for the tracking routine based on pattern recognition, and Hartmut Wolf for the mechanical engineering of the various condenser parts.

References

Allen, R.D., Allen, N.S. & Travis, J.L. (1981) Video-enhanced contrast, differential interference contrast (AVEC-DIC) microscopy: a new method capable of analyzing microtubule-related motility in the reticulopodial network of Allogromia laticollaris. *Cell Motil.* **1**, 291–302.

Allen, R.D., Weiss, D.G., Hayden, J.H., Brown, D.T., Fujiwake, H. & Simpson, M. (1985) Gliding movement of and bidirectional transport along single native microtubules from squid axoplasm: evidence for an active role of microtubules in cytoplasmic transport. *J. Cell Biol.* **100**, 1736–1752.

Benavides, J.M. & Webb, R.H. (2005) Optical characterization of ultrabright LEDs. *Appl. Opt.* **44**, 4000–4003.

Boreal.com (2006) URL http://boreal.com St. Catharines, Ontario.

Carter, N. & Cross, R. (2001) An improved microscope for bead and surface-based motility assays. *Meth. Mol. Biol.* **164**, 73–89.

Dogterom, M. & Yurke, B. (1997) Measurement of the force-velocity relation for growing microtubules. *Science* **278**(5339), 856–860.

Fygenson, D.K., Braun, E. & Libchaber, A. (1994) Phase diagram of microtubules. *Phys. Rev. E,* **50**(2), 1579–1588.

Goetz, W. (2003) White Light (Illumination) with LEDs. Fifth International Conference on Nitride Semiconductors, ICNS-5In, Nara, Japan May 2003.

Gross, H. (2005) 7.4 Diodes. *Handbook of Optical Systems*, p.293. Wiley-VCH, Weinheim, Germany.

Haseloff, J. (2003) URL http://www.plantsci.cam.ac.uk/Haseloff/imaging/cheaposcope/cheaposcope.htm Last checked in January 2007. Department of Plant Science. University of Cambridge, Cambridge, UK.

Herman, P., Maliwal, B.P., Lin, H.J. & Lakowicz, J.R. (2001) Frequency-domain fluorescence microscopy with the LED as a light source. *J. Microsc.* **203**, 176–181.

Inoue, S.(1981) Video image processing greatly enhances contrast, quality, and speed in polarization-based microscopy. *J. Cell Biol.* **89**, 346–356.

Inoue, S.(1989) Imaging of unresolved objects, superresolution, and precision of distance measurement with video microscopy. *Methods Cell Biol.* **30**, 85–112.

Inoue, S. & Spring, K.R. (1997) 3.2. Light sources and microscope image brightness. *Video Microscopy*, pp. 125–130. Plenum, New York.

Kinoshita, K., Arnal, I., Desai, A., Drechsel, D.N. & Hyman, A.A. (2001) Reconstitution of physiological microtubule dynamics using purified components. *Science* **294**(5545), 1340–1343.

Labvision (2005) URL http://www.labvision.com/pdf/fraen.pdf

Mitchison, T. & Kirschner, M. (1984) Dynamic instability of microtubule growth. *Nature* **312**, 237–242.

Moser, C., Mayr, T. & Klimant, I. (2006) Filter cubes with built-in ultrabright light-emitting diodes as exchangeable excitation light sources in fluorescence microscopy. *J. Microsc.* **222**, 135–140.

Neuman, K.C. & Block, S.M. (2004) Optical trapping. *Rev. Sci. Inst.* **75**(9), 2787–2809.

Salmon, E.D. (1995) VE-DIC light microscopy and the discovery of kinesin Trends. *Cell Biol.* **5**, 154–158.

Salmon, E.D. & Tran, P. (1998) High-resolution video-enhanced differential interference contrast (VE-DIC) light microscopy. *Meth. Cell Biol.* **56**, 153–184.

Schäffer, E., Norrelykke, S.F. & Howard, J. (2007) Surface forces and drag coefficients of microspheres near a plane surface measured with optical tweezers. Submitted for publication.

Silk, E. (2002) LED fluorescence microscopy in theory and practice. *Microscope* **50**, 101–118.

Zeiss (2005), Axio Imager. A1 with LED Zeiss, Germany.